Dhaka Univ. J. Sci. 69(3): 125-132, 2022 (June)
Centennial Special Issue

ISSN 1022 - 2502, E-ISSN 2408-8528
DOI: https://doi.org/10.3329/dujs.v69i3.60021

The Effect of Temperature and Solvents on the Thermodynamical and Electronic Properties of N-acetyl-para-aminophenol (APAP): A Computational Study

Md. Alauddin*

Department of Theoretical and Computational Chemistry, University of Dhaka, Dhaka-1000, Bangladesh

(Received : 12 September 2021 ; Accepted: 14 February 2022)

Abstract

Effects of temperature and solvents on the thermodynamical and electronic properties of N-acetyl-para-aminophenol (APAP) have been investigated using density functional theory (DFT) and time dependent density functional theory (TD-DFT). Calculated results shows that thermodynamic properties such as enthalpy (H), entropy (S) and specific heat capacity (C_v) are increased by the raising of temperature (100 K-1200 K) because of enhancing the intensities of molecular vibration. On the contrary, change of Gibb's free energy (ΔG) has been decreased with the increase of temperature. FMO energy gap is enlarged by solvation and therefore APAP becomes more stable in solution especially in polar solvents. Moreover, solvation increases the magnitude of ionization potential, electron affinity, electronegativity, chemical potential and global hardness. Two UV absorption maxima (λ_{max1} and λ_{max2}) are found at 243.08 nm and 193.85 nm which are originated from phenyl and amide chromophore, respectively. The calculated λ_{max1} and λ_{max2} agree quite well with the available experimental data. On the other hand, calculated results reveal that solvation blueshifts the electronic absorption spectraas well as enhances the absorption intensity significantly.

Keywords: Paracetamol, DFT, TDDFT, UV-Vis, Effect of temperature and solvents.

I. Introduction

N-acetyl-para-aminophenol (APAP) is a renownedaniline-based drugs belongs to the class of non-steroid anti-inflammatory drugs (NSAID) and is commercially known as paracetamol in Europe and acetaminophen in USA[1-3].The main advantages for the uses of APAP are low toxicity and low ability for the formation of methemoglobin, a stable oxidized form of hemoglobin which is unable to release oxygen to the tissues. It has also no gastrointestinal toxicity and does not cause thrombocyte aggregation [2]. It is recommended and approved medicine for analgesic to the treatment of children by WHO and FDA[2].APAP possesses analgesics, antipyretic and week anti-inflammatory properties. Therefore, it is commonly used to the relief of fever and headache. Except these,it also used to treat many other conditions such as muscle aches, mild arthritis, chronic low backpain, toothaches, colds, postoperative pain and so on[4-6]. The mechanism for the action of APAP in the metabolic system is the inhibition of cyclo-oxygenase (COX)[7], an enzyme which leads to the production of prostaglandins (PGs) that cause inflammation, swelling, pain and fever [8-9]. Although the uses of APAPhave several merits, however, it has also some demerits depending on type and nature of unusual physical condition of the body and on the limit of dose. Long term use of APAP and overdoses can cause damage of liver and kidney[10].

Numerous experimental works have been done on APAP to understand the structure, structural assignment and stability[11-13], the mechanism of action[14-15], photocatalytic degradation[16-17], method validation for quantitative determination[18-20], to improve analgesic and antipyretic activities and to reduce side effect[21]and applications in prevention of metal corrosion from acid rain[22]. Compared to experimental works, there is no so many computational research yet on APAP. Recently, several computational research works have been performed on APAP to investigate structural stability and reactivity, vibrational assignment, binding affinity and interactions with metal complexes, physicochemical properties (free energy, enthalpy, dipole moment, electrostatic potential, HOMO–LUMO gap, ionization potential, electron affinity, hardness, softness and atomic partial charge) and pharmacokinetics using density functional theory (DFT)[2,3,23,24]. The theoretical analysis of chemical reactivity parameters showed thatparacetamol-oxalic acid cocrystal is more active than paracetamol[25].Very recently, it has been reported from the theoretical work that the expired paracetamol can prevent corrosion of copper from acidrain[22]. However, so far of our knowledge, there is no computational work has been performed on APAP regarding temperature and solvents effect.Therefore, we attempt to investigate the effect of temperature (100 K- 1200 K) and solvents (polar protic, aprotic and non-polar solvents) on the thermodynamicand electronic properties of APAP.

*Author for correspondence. e-mail: alauddin1982@du.ac.bd

II. Methodology

The molecular modeling of APAP were performed using Gaussian16 computational package [26] and the output files were visualized by means of *GaussView* 6.0 software. Frequency calculation showed no imaginary frequencies which assure the minimum energy structure. Density functional theory (DFT) method combined with long range corrected functional includes empirical dispersion (*w*B97XD) using the more accurate basis set of aug-cc-pVTZ were used to compute all the calculations in the gas phase. Moreover, temperature (100 K-1200 K) dependance calculations were also performed using same level of theory. On the other hand, to observe the effects of different types of solvents, implicit solvent effects were modelled using the integral equation formulism variant polarizable continuum model (IEF-PCM) as implement in the Gaussian16 program. The UV-Visible spectra, the electronic properties like frontier molecular orbitals (HOMO, highest occupied molecular orbitals and LUMO, lowest unoccupied molecular orbital) were calculated with the aid of time dependent density functional theory (TD-DFT) approach. The absorption maxima, oscillator strength, energy of HOMO and LUMO, HOMO-LUMO energy gap, major and minor molecular orbital contributions (%) in electronic transitions are identified with the help of GaussSum 3.0 software[27].

III. Results and Discussion

Optimized molecular geometry and thermodynamical parameters at different temperatures

The conformational analysis has been performed to find out the most stable conformers of APAP utilizing DFT/*w*B97XD/aug-cc-pVTZ level of computational approach. Calculation predicted that the trans-conformer is the most stable conformer in which the amino hydrogen atom and the carbonyl group are in opposite direction and are shown in Fig.1.The effect of temperature on the thermodynamic parameters have been simulated using Gaussian 16.0 program package where default temperature and pressure are 298.15 K and 1 atmosphere respectively.

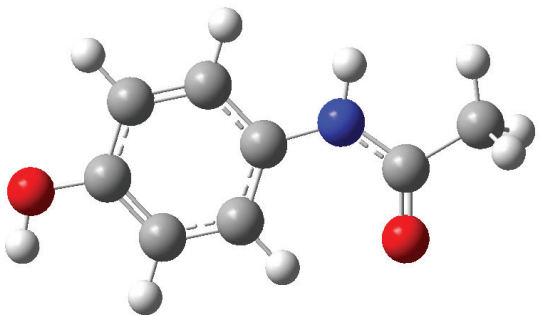

Fig. 1. Optimized molecular structure of the most stable conformer of N-acetyl-para-aminophenol (APAP), also known as paracetamol in Europe and as acetaminophen in USA.

Selected thermodynamic parameters such as Gibb's free energy (G), enthalpy (H), entropy (S) and specific heat capacity (Cv) at constant volume are computed in the range of 100 K to 1200 K to examine the effect of temperature and calculated data are displayed in Table 1. Thermodynamic parameters for the studied compound correlate well with the temperature showing graphs as represented in Fig. 2. The correlation fitting equation among G, H, S and Cvvaries with temperatures were fitted by quadratic formulas and the fitting equations with regression factors (R2) are obtained using Origin 16 software. The thermodynamic correlation fitting equations are given below-

Table 1. Temperature dependence selected thermodynamic parameters of paracetamol (N-acetyl-para-aminophenol) calculated at the DFT/wB97XD/aug-cc-pVTZ level of theory.

Tem-perature /K	Gibb's free energy, G (kcal/mol)	Enthalpy, H (kcal/mol)	Entropy, S (cal/mol-Kelvin)	Specific heat capacity, Cv (cal/mol-Kelvin)
100	94.941	102.188	72.468	16.059
200	86.878	104.525	88.232	26.966
298.15	77.540	107.924	101.910	38.313
400	66.471	112.603	115.330	49.374
500	54.309	118.217	127.818	58.623
600	40.933	124.668	139.560	66.175
700	26.422	131.802	150.544	72.320
800	10.849	139.493	160.808	77.382
900	-5.717	147.648	170.408	81.617
1000	-23.213	156.192	179.407	85.204
1100	-41.580	165.069	187.865	88.270
1200	-60.769	174.229	195.834	90.908

$$G = 103.1672 - 0.07074T - 5.52855 \times E^{-5}\, T^2 \quad (R^2 = 0.99993)$$

$$H = 98.49129 + 0.0239T + 3.32772 \times E^{-5}\, T^2 \quad (R^2 = 0.99922)$$

$$S = 57.68856 + 0.15795T - 3.59792 \times E^{-5}\, T^2 \quad (R^2 = 0.99992)$$

$$C_v = 2.71186 + 0.13651T - 5.32134 \times E^{-5}\, T^2 \quad (R2 = 0.99903)$$

Calculated data reveal that the enthalpies are increased slowly in low temperature region and are raised more steeply in high temperature region. As we know that only translation parts of motion contribute in low temperature but rotational and vibrational motions are excited as temperature increases.

On the contrary, the change of entropy (ΔS) computed have been raised because the energy getting from the temperature distributed rapidly to the translational, rotational and vibrational modes. The change of specific heat capacity (ΔC_v)changes gradually in low temperature and eventually going to be flat in the higher temperature. This depicts that beyond the certain value of temperature (>900 K),

molecular motion is not increased and therefore specific heat capacity at constant volume becomes almost constant. Gibb's free energy is a very important thermodynamic parameter that lessens at the rise of temperature. As we know that the change in Gibb's free energy (ΔG) depends on minus temperature (T) times the change in entropy (ΔS). Therefore, calculated ΔG have been decreased as the entropy increases with increasing temperature.

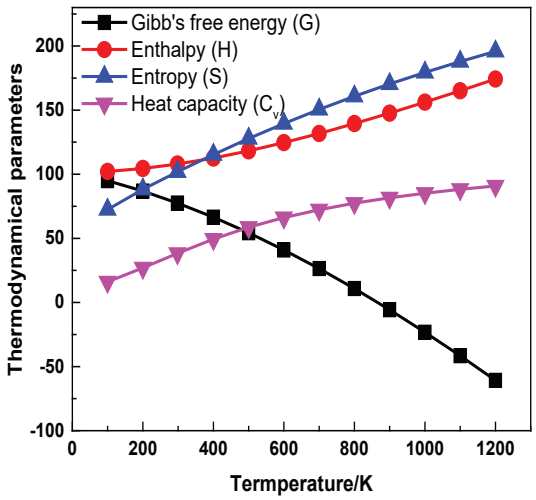

Fig. 2. Graphs representing the dependency of Gibb's free energy (G), enthalpy (H), entropy (S) and specific heat capacity (Cv) at different temperatures (100 K-1200K) for the most stable conformer of N-acetyl-para-aminophenol.

Electronic properties of APAP in gas and in different solvents

Molecular orbitals that are situated in the minimum energy gap in the molecular orbital diagram are designated as frontier molecular orbitals (FMOs) and they are so called highest occupied molecular orbital, in shortly HOMO and lowest unoccupied molecular orbital, in shortly LUMO. The HOMO energy analyzes the ability to donate an electron and the LUMO energy analyzes the ability to gain an electron and HOMO-LUMO energy gap characterizes optical properties, chemical stability and reactivity ofthe molecule[28,29]. Therefore, TD-DFT calculations have been performed to predict the electronic transitions of APAP molecule. Ten lowest singlet excited states are calculated using TD-DFT/*w*B97XD/aug-cc-pVTZ level of computational approach in the gas phase. As well as different type of solvents such as polar protic solvents (water, methanol and ethanol), polar aprotic solvents (dichloromethane (DCM), tetrahydrofuran (THF), acetonitrile, acetone and dimethyl sulfoxide (DMSO)) and non-polar solvents (diethyl ether, CCl_4, benzene, chlorobenzene, toluene and chloroform) were chosen to understand the effect of environmental polarity on FMOs and electronic absorption spectra. Not only that solvation can explore the molecular dipole moment which is also a very important thermochemical property. It is well established that the magnitude of molecular dipole moment in solvent phase is larger compared to the gas phase and depends on the polarity of solvents [30].The absorption maxima (λ_{max}), oscillator strengths (f), energy of HOMO and LUMO, HOMO-LUMO energy gap and molecular dipole moment (μ) have been computed with TD-DFT/*w*B97XD/aug-cc-pVTZ computational method using IEF-PCM solvation model. The data obtained from calculation in different type of solvents having different polarities are presented in Table 2. The energy of HOMO, LUMO and HOMO-LUMO gap were calculated as -7.44 eV, 0.65 eV and 8.09 eV, respectively in the gas phase. FMOs energy gap indicates that APAP is a highly stable compound and less reactive. On the other hand, solvents have significant effect on the FMOs energies and energy gap. DFT-calculated HOMO-LUMO energy gap for polar protic, polar aprotic and non-polar solvents are 8.68 eV, ~8.67 eV and ~8.56 eV, respectively. This results clearly demonstrates that solvation makes APAP molecule highly stable and less reactive. Especially polar protic solvents (water, methanol and ethanol) have significant role to increase the stability of APAP compared to the polar aprotic and non-polar solvents. Consequently, calculated results shows that molecular dipole moment in gas phase is lower compared to the solvent phase. The calculated dipole moment in polar protic, polar aprotic, non-polar solvents and in gas are ~3.232, ~3.220, 2.773 and 2.273 D, respectively. This results clearly demonstrates that polar solvents (protic or aprotic) increase dipole moment whereas non-polar solvents have no effect. Because charge delocalization increases due to the presence of polar solvents and therefore induces the dipole moments raised[30].

Table 2. DFT-calculated absorption maxima, λ_{max} (oscillator strength in parentheses), energy of HOMO, LUMO, HOMO-LUMO (H-L) gap and dipole moment of paracetamol (N-acetyl-para-aminophenol) at various solvents.

Types of solvents	Name of Solvents	λ_{max1} /nm	λ_{max2} /nm	Energy of HOMO /eV	Energy of LUMO /eV	H-L energy gap /eV	Dipole moment, μ /D
No solvent	Gas	243.08 (0.3465)	193.85 (0.3155)	-7.44	0.65	8.09	2.273
Polar protic	Methanol	233.37 (0.4839)	194.86 (0.2815)	-7.85	0.83	8.68	3.227
	Water	233.42 (0.486)	194.87 (0.2818)	-7.85	0.83	8.68	3.263
	Ethanol	233.57 (0.4906)	194.97 (0.2884)	-7.85	0.83	8.68	3.208
Polar aprotic	Acetonitrile	233.81 (0.4923)	194.84 (0.2927)	-7.87	0.83	8.70	3.340
	DCM	233.87 (0.5000)	195.19 (0.3024)	-7.83	0.82	8.65	3.079
	Acetone	233.88 (0.4943)	194.89 (0.2962)	-7.86	0.83	8.69	3.298
	DMSO	233.93 (0.5035)	195.16 (0.2985)	-7.85	0.83	8.68	3.246
	THF	234.08 (0.4995)	195.08 (0.3064)	-7.84	0.81	8.65	3.141
Non-polar	Diethyl ether	233.34 (0.4795)	194.98 (0.2903)	-7.81	0.79	8.60	2.895
	CCl_4	233.82 (0.4933)	195.46 (0.3113)	-7.78	0.75	8.53	2.655
	Chloroform	233.91 (0.4995)	195.29 (0.3079)	-7.81	0.80	8.61	2.927
	Benzene	233.04 (0.5009)	195.59 (0.3184)	-7.79	0.75	8.54	2.663
	Cyclohexane	233.61 (0.4856)	195.38 (0.305)	-7.78	0.73	8.51	2.611
	Toluene	234.02 (0.5007)	195.56 (0.3175)	-7.79	0.75	8.54	2.682
	Chlorobenzene	234.35 (0.5154)	195.52 (0.3206)	-7.82	0.81	8.63	2.979

The important parameters namely the ionization potential (I), electron affinity (A), chemical potential (μ), absolute electronegativity (χ), hardness (η), softness (S) and electrophilicity index (ω) which are known as global chemical reactivity descriptors (GCRD) are strongly depends on FMOs. All these parameters are computed on the basis of HOMO and LUMO energy formulating Koopman's theorem[31] for closed-shell molecules-

$$\chi = \left(\frac{I+A}{2}\right),\ \eta = \left(\frac{I-A}{2}\right),\ \mu = -\left(\frac{I+A}{2}\right),$$

$$S = \frac{1}{2\eta}\ ,\ \omega = \frac{\mu^2}{2\eta}$$

Where, I (ionization potential) is the energy of HOMO and A (electron affinity) is the energy of LUMO. The GCRD values obtained from calculation in different type of solvents having different polarities are listed in Table 3. The predicted value of ionization potential for gas, polar protic solvents, polar aprotic solvents and non-polar solvents are 7.44, 7.85, ~7.85 and ~7.79 eV, respectively. This means ionization potential have been increased by solvation. The magnitude of electron affinity has also been increased by solvation. The value of electronegativity has been increased slightly by solvation compared to the gas phase which confirm that APAP molecule would be energetically favored for electrophilic attack[32].

Table 3. Global reactivity descriptors of the most stable conformer of paracetamol (N-acetyl-para-aminophenol) with wB97XD/aug-cc-pVTZ computational approach.

Types of solvents	Name of Solvents	Ionization Potential (I)/eV	Electron Affinity (A)/eV	Electronegativity (χ)/eV	Chemical Potential (μ)/eV	Global Hardness (η)/eV	Softness (S)/eV	Electrophilicity Index (ω)/eV
No solvent	Gas	7.44	-0.65	3.40	-3.40	4.05	0.124	1.425
	Methanol	7.85	-0.83	3.51	-3.51	4.34	0.115	1.419
Polar protic	Water	7.85	-0.83	3.51	-3.51	4.34	0.115	1.419
	Ethanol	7.85	-0.83	3.51	-3.51	4.34	0.115	1.419
	Acetonitrile	7.87	-0.83	3.52	-3.52	4.35	0.115	1.424
	DCM	7.83	-0.82	3.51	-3.51	4.33	0.116	1.420
Polar aprotic	Acetone	7.86	-0.83	3.52	-3.52	4.35	0.115	1.422
	DMSO	7.85	-0.83	3.51	-3.51	4.34	0.115	1.419
	THF	7.84	-0.81	3.52	-3.52	4.33	0.116	1.428
	Diethyl ether	7.81	-0.79	3.51	-3.51	4.30	0.116	1.433
	CCl_4	7.78	-0.75	3.52	-3.52	4.27	0.117	1.448
	Chloroform	7.81	-0.80	3.51	-3.51	4.31	0.116	1.427
Non-polar	Benzene	7.79	-0.75	3.52	-3.52	4.27	0.117	1.451
	Cyclohexane	7.78	-0.73	3.53	-3.53	4.26	0.118	1.460
	Toluene	7.79	-0.75	3.52	-3.52	4.27	0.117	1.451
	Chlorobenzene	7.82	-0.81	3.51	-3.51	4.32	0.116	1.424

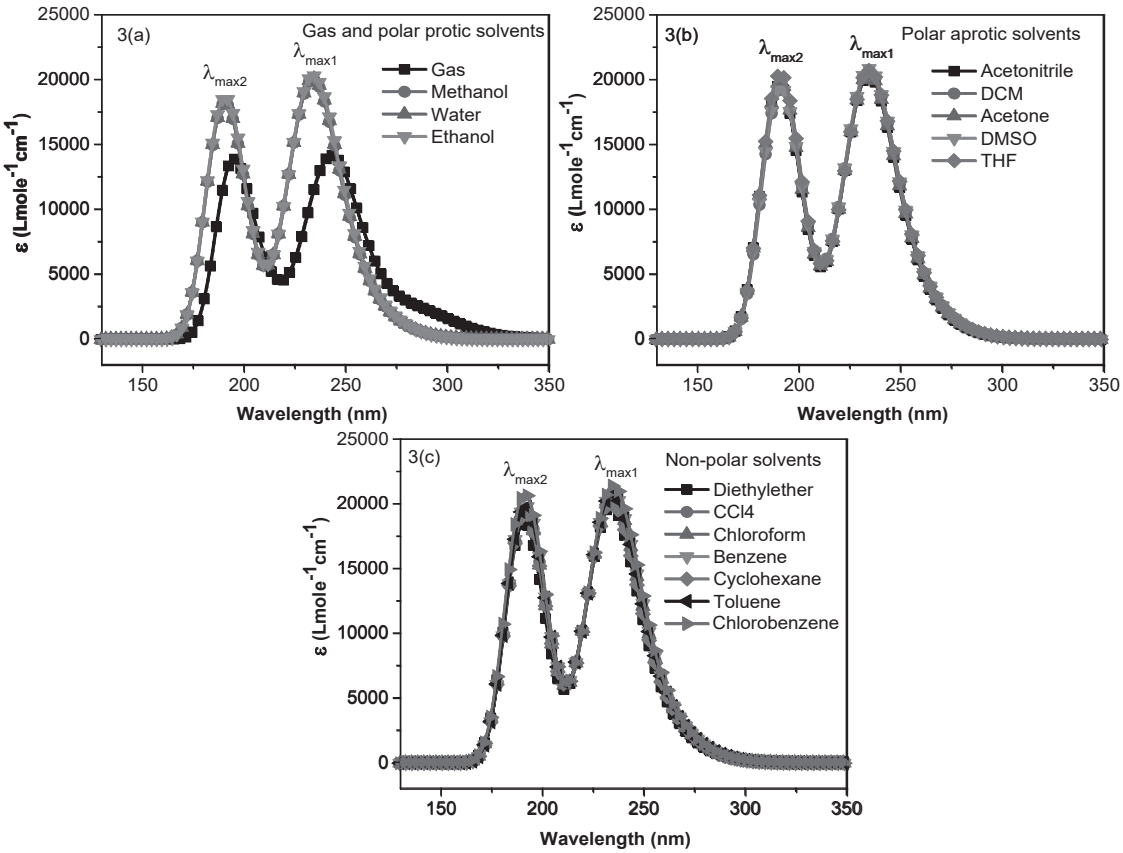

Fig. 3. DFT-calculated UV spectra of the most stable conformer of paracetamol (N-acetyl-para-aminophenol) at various solvents: 3(a) gas and polar protic solvents, 3(b) polar aprotic solvents and 3(c) non-polar solvents.

Two global descriptors such as chemical hardness and softness are very importantas they are taken into account to indicate transformation of charge within a molecule. The molecules that have large energy gap are called hard molecules whereas it is soft if energy gap is small. Consequently, soft molecules have higher polarizability than hard ones since minimum amount of energy are required for transition[30]. Upon solvation, calculated values of hardness are increased whereas softness decreased. The value of very low chemical softness of 0.124 (gas) and of 0.115 (solution) tells the trans-conformer of APAP is non-toxic compound. Non-polar solvents enhance electrophilicity index significantly compared to the polar solvents and gas. Although APAP has very low electrophilicity index with a value of 1.425 eV.

The UV-Visible absorption spectra calculated forAPAP in gas and in different solvents are presented in Fig. 3.

wTwo absorption maxima ($\lambda_{max1}$and λ_{max2}) were found both in gas phase and in solvent phase.The 1st absorption maxima (λ_{max1}) was appeared at 243.08 nm with oscillator strength of 0.3465 that arises from phenyl chromophore basically π to π* transition. The 2nd absorption maxima (λ_{max2}) was appeared at 193.85 nm with oscillator strength of 0.3155 which arises from the amide chromophore N-C=O (n to π* transition). On the other hand, λ_{max1} and λ_{max2} were found at around 233 nm (5.322 eV) and 194 nm (6.391 eV) respectively for polar protic, aprotic and non-polar solvents. As we know that solvation increases the excitation energies and induces blue shift in the electronic spectrum[33,34]. Solvation blueshifted the electronic spectrum and also enhanced oscillator strength (f) significantly. However, the polarity of the solvents (polar protic, aprotic and non-polar) has no significant effect.

Table 4. Calculated UV spectra and assignments for the ten lowest excited states of paracetamol (N-acetyl-para-aminophenol) via photoexcitation process using TD-DFT/wB97XD/aug-cc-pVTZcomputational approach.

Expt. (nm)	λ (nm)	Transition states	Nature of transitions	Oscillator Strength (f)	Energy (eV)	Assignment	
						Major contribution (≥ 10%)	Minor contribution (≤ 10 %)
243	284.03	$S_0 \rightarrow S_1$	π →σ*	0.0537	4.3653	HOMO->L+3 (83%)	H-1->L+7 (5%), HOMO->L+4 (6%), HOMO->L+7 (3%)
	243.08	$S_0 \rightarrow S_2$	π→π*	0.3465	5.1006	HOMO->L+7 (86%)	H-1->L+3 (5%), HOMO->L+4 (3%)
	243.03	$S_0 \rightarrow S_3$	n→π*	0.0001	5.1015	HOMO->LUMO (64%), HOMO->L+1 (11%)	HOMO->L+2 (3%), HOMO->L+6 (3%), HOMO->L+9 (4%), HOMO->L+11 (3%), HOMO->L+16 (4%)
	234.62	$S_0 \rightarrow S_4$	π→π*	0.0002	5.2845	HOMO->L+1 (67%)	HOMO->LUMO (7%), HOMO->L+2 (3%), HOMO->L+10 (4%), HOMO->L+13 (6%), HOMO->L+14 (5%)
	223.65	$S_0 \rightarrow S_5$	σ→π*	0.0009	5.5437	H-2->L+7 (59%) H-2->L+12 (12%)	H-2->L+4 (9%), H-2->L+15 (9%), H-2->L+19 (5%)
	209.62	$S_0 \rightarrow S_6$	π→π*	0.0009	5.9148	HOMO->L+2 (65%), HOMO->L+5 (16%)	HOMO->L+9 (3%), HOMO->L+17 (5%)
	208.46	$S_0 \rightarrow S_7$	π →σ*	0.0846	5.9476	HOMO->L+4 (54%), HOMO->L+12 (24%)	H-1->L+3 (6%), HOMO->L+3 (6%)
	204.95	$S_0 \rightarrow S_8$	π →σ*	0.0001	6.0495	HOMO->L+6 (55%)	HOMO->L+5 (4%), HOMO->L+8 (7%), HOMO->L+10 (9%), HOMO->L+11 (3%), HOMO->L+14 (6%), HOMO->L+24 (4%)
	198.50	$S_0 \rightarrow S_9$	n →π*	0.0001	6.2459	HOMO->L+5 (28%), HOMO->L+6 (17%), HOMO->L+9 (14%)	HOMO->L+11 (10%) HOMO->L+1 (2%), HOMO->L+2 (3%), HOMO->L+8 (5%), HOMO->L+10 (4%), HOMO->L+17 (3%), HOMO->L+20 (4%)
~190	193.85	$S_0 \rightarrow S_{10}$	n →π*	0.3155	6.3960	H-1->L+3 (56%), HOMO->L+4 (12%)	H-3->L+7 (2%), H-1->L+4 (5%), HOMO->L+7 (7%), HOMO->L+15 (6%), HOMO->L+18 (6%)

Ten lowest singlet excited states are calculated using TD-DFT/*w*B97XD/aug-cc-pVTZ level of computational method in the gas phase. The absorption wavelengths (λ), energy of excitation (E), oscillator strengths (f), excited state, nature of transition, major and minor contributions of molecular orbitals and assignments of the electronic transitions are defined with the help of Gauss-Sum 3.0 software and listed in Table 4. As well as experimental absorption wavelength are included in the Table 4 for comparison. It is well known that the electronic absorption varies depending on the nature of ground and the first electronic state. Basically, it is designated by the photoexcitation of electrons from HOMO to LUMO. The first electronic transition is observed at 284.03 nm (4.365 eV) with oscillator strength of 0.0537. This transition is originated from the ground state to the first singlet excited state ($S_1 \leftarrow S_0$) and the major excitation corresponds from HOMO to L+3 with orbital contribution of 83% that leading to a transition character of π to σ*. In addition, there are some other minor excitations occurs from H-1 to LUMO, HOMO to L+4 and HOMO to L+7 with contribution of 5%, 6% and 3% respectively. The second electronic transition ($S_2 \leftarrow S_0$) is predicted at 243.08 nm (5.101 eV) with the highest oscillator strength of 0.3465. The main electronic transition occurs from HOMO to L+7 with orbital contribution of 86% and the nature of electronic excitation is π to π*. Some other transitions such as H-1 to L+3 (5%) and HOMO to L+4 (3%) are also contributed to the appeared spectrum. It is interesting that calculated absorption spectra at 243.08 nm agree very well with the experimental absorption spectrum (243 nm)[35].

The third electronic transition ($S_3 \leftarrow S_0$) is observed at 243.03 nm (5.102 eV) with very weak oscillator strength of 0.0001. This excitation originated mainly form HOMO to LUMO (64%) and HOMO to L+1 (11%) and the nature of electronic transition from n to π*. The predicted fourth electronic transition ($S_4 \leftarrow S_0$) is found at 234.62 nm (5.284 eV) with very weak oscillator strength of 0.0002. This transition is originated from π to π* with orbital contribution of HOMO to L+1 (67%). The fifth and sixth electronic transitions are found at 223.65 nm (5.284 eV) and 209.62 nm (5.543 eV) with the same oscillator strength of 0.0009. The fifth transition arises from σ to π* with major molecular orbital contribution of HOMO to L+7 (59%) and sixth transition arises from π to π* with orbital contribution of HOMO to L+2 (65%). The 7th, 8th and 9th transitions are originated from π to σ*, π to σ*, n →π* and predicted at 208.46 nm, 204.95 nm and 198.50 nm, respectively. H to L+4 (54%), H to L+6 (55%) and H to L+5/6/9 (59%) orbital contributions are participated in the 7th, 8th and 9th transition respectively.

The tenth electronic transition ($S_{10} \leftarrow S_0$) is predicted at 193.85 nm (6.396 eV) with strong oscillator strength of 0.3155. The major excitation corresponds from H-1 to L+3 with orbital contribution of 63% that leading to a transition character of n to π*. In addition, there are several minor transitions that are also contributed. The experimental λ_{max2} (~190 nm)[35] matches quiet well with the calculated one.

IV. Conclusion

Quantum chemical calculations have been performed to investigate the effect of temperature (100 K-1200 K) and solvents (polar protic, aprotic and non-polar solvents) on the thermodynamical and electronic properties of APAP. The calculated thermochemical data predicted that the value of H, S and Cv are increased with the increase of temperature because the energy getting from the temperature distributed rapidly to the translational, rotational and vibrational modes. The APAP compound is a very stable and less reactive as the computed HOMO-LUMO energy gap is 8.09 eV which is high. But the solvation increases FMO energy gap and therefore the APAP become more stable in solution especially in polar solvents. Consequently, the solvation also increases the values of I, A, μ, χ and η. The value of very low chemical softness of 0.124 (gas) and of 0.115 (solution) confirms that the solvation makes APAP molecule more non-toxic. Two strong absorption bands are found in gas phase as well as in solvent phase. The λ_{max1} was appeared at 243.08 nm that arises from phenyl chromophore with electronic transition of π to π* and the λ_{max2}(at 193.85 nm) that arises from the amide chromophore N-C=O with a transition character of n to π*. The calculated UV absorption maxima (λ_{max1} and λ_{max2}) agree quite well with the available experimental spectra. Finally, electronic absorption spectra become blueshifted and enhanced intensity significantly by solvation but the polarity of the solvents has no specialty.

References

1. Thybo, K. H., D. Hägi-Pedersen, J. Wetterslev, J. B. Dahl, H. M. Schrøder, H. H. Bülow, J. G. Bjørck and O. Mathiesen, 2017. PANSAID – Paracetamol and NSAID in combination: study protocol for a randomised trial. *Trials*, **18(11)**, 1749-7.
2. Syrovaya, A. O., O. L. Levashova and S. V. Andreeva, 2015. Investigation of quantum-chemical properties of paracetamol.*J. Chem. Pharm. Res.***7(1)**, 307-311.
3. Ahmed, L. O. and R. A. Omer, 2020. Computational Study on Paracetamol Drug.*J. Phys. Chem. Funct. Mater.***3(1)**, 9-13.
4. Hossen, M. B., Z. A. Siddique, M. U. Zaman, A. Ahsan and M. K. U. Chowdhury, 2019. A Computational Approach to Investigate the Biochemical Properties of Paracetamol and Its Metabolites. *Biomed. J. Sci.& Tech. Res.***22 (4)**, 16860-16865.
5. Bertolini, A. A. Ferrari, A. Ottani, S. Guerzoni, R. Tacchi, S. Leone, 2006. Paracetamol: New Vistas of an Old Drug.*CNS Drug Rev.***12 (3-4)**, 250-275.
6. Ong, C. K. S., R. A. Seymour, P. Lirkand A. F. Merry, 2010. Combining Paracetamol (Acetaminophen) with Nonsteroidal Antiinflammatory Drugs: A Qualitative Systematic Review of Analgesic Efficacy for Acute Postoperative Pain.*Anesth. Analg.***110**, 1170–9.
7. Hinz, B. and K. Brune, 2012. Paracetamol and cyclooxygenase inhibition: is there a cause for concern? *Ann. Rheum. Dis.***71**, 20-25.
8. Nørregaard, R., T. H. Kwon and J. Frøkiær, 2015. Physiology and pathophysiology of cyclooxygenase-2 and prostaglandin

E2 in the kidney.*Kidney Res. Clin. Pract.***34**, 194-200.

9. Harris, R. C. and M. Z. Zhang, 2011. Cyclooxygenase Metabolites in the Kidney. *Compr. Physiol.***1**, 1729-1758.
10. McCrae, J. C., E. E. Morrison, M. Maclntyre, J. W. Dear and D. J. Webb, 2018. Long-term adverse effects of paracetamol – a review.*Br. J. Clin. Pharmacol.***84(10)**, 2218-2230.
11. El-Shahawy, A., 2014. DFT Cancer Energy Barrier and Spectral Studies of Aspirin, Paracetamol and Some Analogues. *Comput. Chem.***2**, 6-17.
12. Allen, F. H.,2002. The Cambridge Structural Database: a quarter of a million crystal structures and rising. *ActaCryst.* **B58**, 380-388.
13. Borges, R. S., T. G. Barros, G. A. N. Pereira, J. Batista Jr., R. F. G. P. B. Filho, A. A. S. Veiga, M. Hamoy, V. J. Mello, A. B. F. da Silva and C. A. L. Barros, 2014. A Structure and Antioxidant Activity Study of Paracetamol and Salicylic Acid. *Pharmacol. Pharm.***5**, 1185-1191.
14. Sharma, C. V. and V. Mehta, 2014. Paracetamol: mechanisms and updates. *Continuing Education in Anaesthesia Critical Care & Pain*, **14 (4),** 153-158.
15. Alves, C. N., R. S. Borges and A. B. F. da Silva, 2006. Density Functional Theory Study of Metabolic Derivatives of the Oxidation of Paracetamol. *Int. J. Quantum Chem.***106**, 2617-2623.
16. Jallouli, N., K. Elghniji, H. Trebelsi and M. Ksibi, 2017. Photocatalytic degradation of paracetamol on TiO2 nanoparticles and TiO2/cellulosic fiber under UV and sunlight irradiation. *Arab. J. Chem.***10**, S3640–S3645.
17. Granados, B. L., R. S. Tovar, R. M. F. Domene and J. G. Anton, 2019. A pH Study for the Degradation of Acetaminophen with Iron Oxide Nanostructures.*Chem. Eng. Trans.***73**, 139-144.
18. Saeed, A. M. and N. Q. Ahmed, 2017. Estimation of Paracetamol, Aspirin, Ibuprofen, Codeine and Caffeine in some Formulated Commercial Dosage using UV – Spectroscopic Method. *Eur. J. Pharma. Med. Res.***4(7),** 33-38.
19. Glavanovic, S., M. Glavanovic and V. Tomisic, 2016. Simultaneous quantitative determination of paracetamol and tramadol in tablet formulation using UV spectrophotometry and chemometric methods. *Spectrochim. Acta A*,**157**, 258-264.
20. Dinc, E., Z. C. Ertekin and N. Unal, 2020. Three-way analysis of pH-UV absorbance dataset for the determination of paracetamol and its pKa value in presence of excipients. *Spectrochim. Acta A*, **230**, 118049.
21. Zaman, M. U., J. Shawon and Z. A. Siddique, 2019. Molecular docking, dynamics simulation and ADMET prediction of Acetaminophen and its modifed derivatives based on quantum calculations. *SN Appl. Sci.***1**, 1437.
22. Tasic, Z. Z., M. B. P. Mihajlovic, M. B. Radovnovic, A. T. Simonovic, M. M. Antonijevic, 2021. Experimental and theoretical studies of paracetamol as a copper corrosion inhibitor. *J. Mol. Liq.* **327**, 114817.
23. Al-Otaibi, J. S.,2016. Quantum Chemical Studies and Electrochemical Investigations of Polymerized Brilliant Blue-Modified Carbon Paste Electrode for In Vitro Sensing of Pharmaceutical Samples. *Int. J. Biol. Pharm. Allied Sci.***5(4)**, 887-899.
24. Ganesh, P. S., S. Y. Kim, S. Kaya, R. Salim, G. Shimoga and S. H. Lee, 2021. Quantum Chemical Studies and Electrochemical Investigations of Polymerized Brilliant Blue-Modified Carbon Paste Electrode for In Vitro Sensing of Pharmaceutical Samples. *Chemosensors*,**9**, 135.
25. Srivastava, K., M. R. Shimpi, A. Srivastava, P. Tandon, K. Sinha and S. P. Velaga, 2016. Vibrational analysis and chemical activity of paracetamol-oxalic acid cocrystal based on monomer and dimer calculations: DFT and AIM approach. *RSC Adv.***6**, 10024-10037.
26. M. J. Frisch, G. W. Trucks, H. B. Schlegel, G. E. Scuseria, M. A. Robb, J. R. Cheeseman, G. Scalmani, V. Barone, G. A. Petersson, H. Nakatsuji, X. Li, M. Caricato, A. V. Marenich, J. Bloino, B. G. Janesko, R. Gomperts, B. Mennucci, H. P. Hratchian, J. V. Ortiz, A. F. Izmaylov, J. L. Sonnenberg, D. Williams-Young, F. Ding, F. Lipparini, F. Egidi, J. Goings, B. Peng, A. Petrone, T. Henderson, D. Ranasinghe, V. G. Zakrzewski, J. Gao, N. Rega, G. Zheng, W. Liang, M. Hada, M. Ehara, K. Toyota, R. Fukuda, J. Hasegawa, M. Ishida, T. Nakajima, Y. Honda, O. Kitao, H. Nakai, T. Vreven, K. Throssell, J. A. Montgomery, Jr., J. E. Peralta, F. Ogliaro, M. J. Bearpark, J. J. Heyd, E. N. Brothers, K. N. Kudin, V. N. Staroverov, T. A. Keith, R. Kobayashi, J. Normand, K. Raghavachari, A. P. Rendell, J. C. Burant, S. S. Iyengar, J. Tomasi, M. Cossi, J. M. Millam, M. Klene, C. Adamo, R. Cammi, J. W. Ochterski, R. L. Martin, K. Morokuma, O. Farkas, J. B. Foresman, and D. J. Fox, **Gaussian 16, Revision B.01**, Gaussian, Inc., Wallingford CT, 2016.
27. O'boyle, N. M., A. L. Tenderholt and K. M. Langner, 2008. Cclib: A Library for Package-Independent Computational Chemistry Algorithms. *J. Comp. Chem.***29**, 839-845.
28. Tao, Y., L. Han, Y. Han and Z. Liu, 2015. Experimental and theoretical studies on the vibrational spectra of trans-3-phenylacryloyl chloride. *Spectrochim. Acta A*,**137**, 892-898.
29. Alturk, S., D. Avci, O. Tamer and Y. Atalay, 2018. 1H-pyrazole-3-carboxylic acid: Experimental and computational study. *J. Mol. Struct.***1164**, 28-36.
30. Kosar, B. and C. Albayrak, 2011. Spectroscopic investigations and quantum chemical computational study of (E)-4-methoxy-2-[(p-tolylimino)methyl] phenol. *Spectrochim. Acta A*, **78**, 160-167.
31. Koopmans, T. A. 1934. Uber Die Zuordnung Von Wellenfunktionen and EigenwertenZu Den, EinzelnenElektronenEines Atoms. *Physica,***1**,104-113.
32. Vijayaraj, R., V. Subramanian and P. K. Chattaraj, 2009. Comparison of Global Reactivity Descriptors Calculated Using Various Density Functionals: A QSAR Perspective. *J. Chem. Theory Comput.***5**, 2744-2753.
33. Bi, T. J., L. K. Xu, F. Wang, M. J. Ming and X. Y. Li, 2017. Solvent effects on excitation energies using state-specific TD-DFT method with polarizable continuum model based on constrained equilibrium thermodynamics. *Phys. Chem. Chem. Phys.***19**, 32242-32252.
34. Hai-Sheng R., Y. K. Li, Q. Zhu, J. Zhu and X. Y. Li, 2012. Spectral shifts of the $n \rightarrow \pi^*$ and $\pi \rightarrow \pi^*$ transitions of uracil based on a modified form of solvent reorganization energy. *Phys. Chem. Chem. Phys.***14**, 13284-13291.
35. Behera, S., S. Ghanty, F. Ahmad, S. Santra and S. Banerjee, 2012. UV-Visible Spectrophotometric Method Development and Validation of Assay of Paracetamol Tablet Formulation. *J. Anal. Bioanal. Tech.***3(6),**151-156.